



## Article

# VLF Signal Noise Reduction during Intense Seismic Activity: First Study of Wave Excitations and Attenuations in the VLF Signal Amplitude

Aleksandra Nina

Institute of Physics Belgrade, University of Belgrade, Pregrevica 118, 11080 Belgrade, Serbia; sandrast@ipb.ac.rs

**Abstract:** This study is a continuation of pilot research on the relationships between seismic activity and changes in very low frequency (VLF) signals starting a few minutes or a few dozen minutes before an earthquake. These changes are recorded in the time and frequency domains and their duration can be influenced not only by the strongest earthquake but also by others that occur in a short time interval. This suggests that there are differences in these changes in cases of individual earthquakes and during the period of intense seismic activity (PISA). In a recent study, they were validated in the time domain by comparing the amplitude noise reductions during the PISA and before earthquakes that occurred in the analysed periods without intense seismic activity (PWISA). Here, we analyse the changes in the VLF signal amplitude in the frequency domain during the PISA and their differences are compared to the previously investigated relevant changes during PWISA. We observe the signal emitted by the ICV transmitter in Italy and received in Serbia from 26 October to 2 November 2016 when 907 earthquakes occurred in Central Italy. The study is based on analyses of the Fourier amplitude  $A_F$  obtained by applying the fast Fourier transform (FFT) to the values of the ICV signal amplitude sampled at 0.1 s. The obtained results confirm the existence of one of the potential earthquake precursors observed during PWISA: significantly smaller values of  $A_F$  for small wave periods (they can be smaller than  $10^{-3}$  dB) than under quiet conditions (the expected values are larger than  $10^{-2}$  dB). Exceptions were the values of  $A_F$  for wave periods between 1.4 s and 2 s from a few days before the observed PISA to almost the end of that period. They were similar or higher than the values expected under quiet conditions. The mentioned decrease lasted throughout the observed longer period from 10 October to 10 November, with occasional normalisation. It was many times longer than the decreases in  $A_F$  around the considered earthquakes during PWISA, which lasted up to several hours. In addition, no significant wave excitations were recorded at discrete small values of the wave periods during the PISA, as was the case for earthquakes during PWISA. These differences indicate the potential possibility of predicting the PISA if the corresponding earthquake precursors are recorded. Due to their importance for potential warning systems, they should be analysed in more detail in future statistical studies.



**Citation:** Nina, A. VLF Signal Noise Reduction during Intense Seismic Activity: First Study of Wave Excitations and Attenuations in the VLF Signal Amplitude. *Remote Sens.* **2024**, *16*, 1330. <https://doi.org/10.3390/rs16081330>

Academic Editors: Yuriy G. Rapoport, Volodymyr Grimalsky, Anatoly Kotsarenko and Gianfranco Cianchini

Received: 1 February 2024

Revised: 4 April 2024

Accepted: 5 April 2024

Published: 10 April 2024

**Keywords:** earthquake precursors; VLF signal; wave excitations/attenuations



**Copyright:** © 2024 by the authors. Licensee MDPI, Basel, Switzerland. This article is an open access article distributed under the terms and conditions of the Creative Commons Attribution (CC BY) license (<https://creativecommons.org/licenses/by/4.0/>).

## 1. Introduction

The decades-long efforts of researchers to find a mechanism for the detection of earthquake precursors have been focused on the investigation of numerous phenomena [1–3]. These include studies of changes in the ionosphere [4–14] and the electromagnetic signals used to monitor it [15–18].

This paper analyses the characteristics of a very low frequency (VLF) radio signal used to monitor the lower ionosphere. As numerous studies show, there are several different changes in the characteristics of VLF and low-frequency (LF) signals that can occur before an earthquake. They are mostly detected a few days or weeks before strong earthquakes [19–21], and are manifested in a significant increase/decrease in the

signal amplitude/phase [22,23], in the shift of the terminator time during sunrise and sunset [8,20,24,25] and in variations in the wavelet power spectrum [22,26]. These investigations are mainly based on amplitude/phase processing of VLF/LF signals sampled with a time interval of not less than 1 s.

In 2020, the first relevant research based on the analysis of VLF signal amplitudes recorded with a time resolution of 0.1 s was published [27]. This improvement in resolution led to the discovery of new potential earthquake precursors observed in the time and frequency domains. In the time domain, the corresponding changes are manifested by reductions in the amplitude and phase noises. In the frequency domain, the analysis of the Fourier amplitude obtained by applying the fast Fourier transform (FFT) to the time evolutions of the signal amplitude and phase shows its increases at discrete low values of wave periods and its decreases at other, also low-value, wave periods. The first investigations of these changes in signal characteristics have been published in several studies [27–31]. One of the basic conclusions is that it is possible to connect several earthquakes that occur in a short time interval in some localised area with one change in the signal, i.e., that several events occur during one continuous disturbance. This has led to the conclusion that the detection of the mentioned changes is influenced by the duration of seismic activity. This has been confirmed in the case of the amplitude noise reduction in the time domain in the analysis of the period of intense seismic activity (PISA) in Central Italy when almost 1000 earthquakes were registered in a period of 10 days. Namely, the results of the study presented in [29] show that one amplitude noise reduction that occurs before one earthquake can continue without normalisation and without additional reductions during the period of occurrence of other earthquakes.

The aim of this research is to examine the changes in the VLF signal amplitude during the seismically active period in the frequency domain, which is a continuation of the analysis of the corresponding changes in the time domain given in [29]. We observe the amplitude characteristics of the ICV signal emitted in Italy and received at the Institute of Physics Belgrade in Belgrade, Serbia. The focus of the analysis is on the eight-day period from 26 October to 2 November 2016. Here, we use the same methods as those described in the studies of earthquakes that occurred during periods without intense seismic activity (PWISA) [27,30]. In addition, the daily values of the parameters relevant to the study during a one-month interval (10 October–10 November 2016) are presented in order to determine the beginnings and endings of the observed changes. Detailed analyses are also conducted for 3 October 2010 and 25 October 2016, which are taken as reference days in the analyses of the considered changes.

This paper is organized as follows. Section 2 describes the events that took place in the observed period and the signal whose characteristics are analysed. The signal processing is explained in Section 3, and the obtained results and their discussion are presented in Section 4. The conclusions of this study are set out in Section 5.

## 2. Observations

According to the data provided on the Euro-Mediterranean Seismological Centre website [32], earthquakes in Central Italy were registered every day (except on 18 October 2016) during a one-month interval from 10 October to 10 November 2016. The total number of earthquakes and the number of earthquakes with a minimum magnitude of four (hereafter referred to as stronger earthquakes) that occurred in that time interval are given in the upper and lower panels of Figure 1, respectively. Here, we note that the magnitudes on the mentioned website are given in the moment magnitude [33], body-wave magnitude [34], and Richter [35] scales. As in the previous relevant studies, here, we considered earthquakes with a minimum magnitude of four on any of these scales and used  $M$  as a common term for all given magnitudes. The obtained time evolutions indicated that the total number of earthquakes increased sharply on 26 October. On that day, six earthquakes of minimum magnitude four were recorded, including earthquakes of magnitudes  $M_w$  5.5 and  $M_w$  6.1. For these reasons, 26 October was the beginning of the

period that was the focus of this study. The highest seismic activity was on 30 October with 268 earthquakes, including 14 stronger earthquakes with a maximum magnitude of Mw 6.5. The calming of the ground tremors in Central Italy after that maximum was slower than its intensification, but the recorded magnitudes were not large. It can be assumed that the series of earthquakes with  $M \geq 4$  ended on 3 October. Namely, only one such earthquake occurred in the following week (on 7 November). Based on this and the fact that the analysed signal was bad during a significant part of 3 October, 2 November was set as the end of the period in which the data that were the focus of this study were recorded.

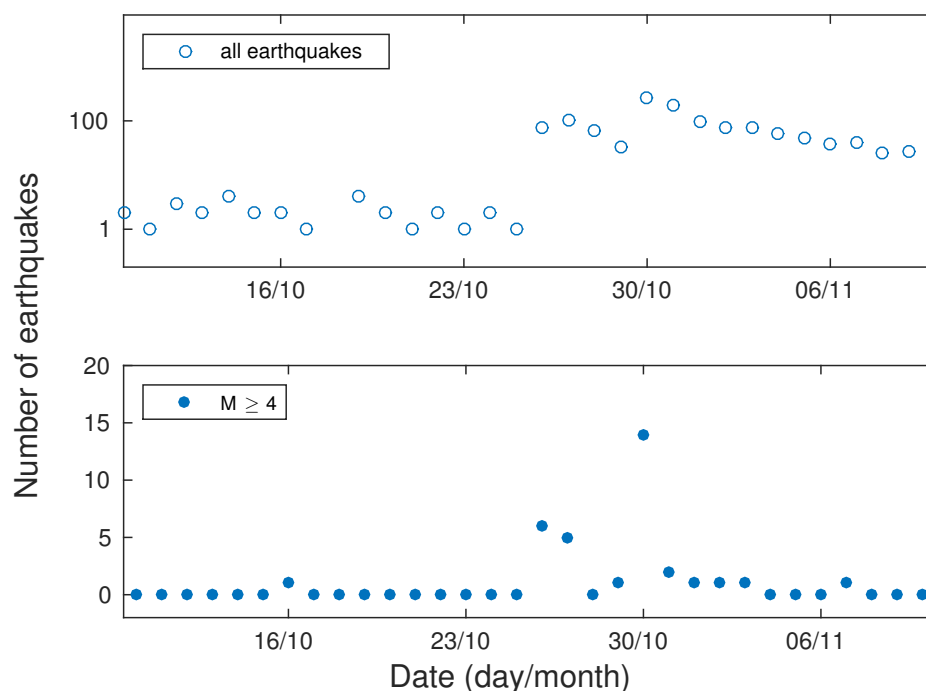


**Figure 1.** The total number of earthquakes (**upper panel**) and earthquakes with minimum magnitude of 4 (**bottom panel**) that occurred in the period from 10 October to 10 November 2016. The displayed data are taken from the Euro-Mediterranean Seismological Centre website [32]. The boxed part indicates the time period considered in detail in this study.

In this study, we used a VLF signal that monitors the low ionosphere to investigate earthquake precursors. The importance of this technique in research of sudden events such as earthquakes lies in the continuous observation of a large area. Namely, it is based on the operation of numerous transmitters and receivers of VLF signals that are distributed all over the world. In addition, the time resolution of the recorded data can be of the order of milliseconds. This ensures (a) the ability to detect short-term changes that last less than 1 s, and (b) the analysis of somewhat longer changes (lasting several seconds or minutes) that require a lot of data during the disturbance period. Otherwise, the receivers can record the electrical or magnetic component of VLF and LF signals, depending on whether the antenna is electrical or magnetic. Some of them record both the amplitude and the phase of the signal, while others record only one of these signal parameters.

As in previous analyses of excitations and attenuations of small-period waves in the time intervals around the considered earthquakes [27,29,30], we examined the changes in the amplitude characteristics of the VLF signal emitted by the ICV transmitter located in Isola di Tavolara, Sardinia, Italy (40.92 N, 9.73 E) and received by the Absolute Phase and Amplitude Logger (AbsPAL) receiver in Belgrade, Serbia (44.8 N, 20.4 E). The ICV transmitter emits at 20.27 kHz with a power of 20 kW. The used receiver (located at the Institute of Physics Belgrade) has an electrical antenna and records both the amplitude and the phase of VLF/LF signals. It can monitor five signals simultaneously and provides

two data sets with time sampling resolutions of 0.1 s and 1 min. In this study, we used the first data set. The route of this signal and the epicentres of all earthquakes that were recorded in its vicinity during the observed time interval are shown in Figure 2. The locations of the epicentres show that they were dominantly concentrated in a localized area in Central Italy. The classification of the considered earthquakes according to their magnitudes is visualised by the different colours of the dots representing the locations of their epicentres (see explanation in the caption of Figure 2). It indicates that only two stronger earthquakes did not occur in Central Italy (they were registered in Bosnia and Herzegovina and Southern Italy). The characteristics of all shown stronger earthquakes are given in Table 1, where the two highlighted in grey are mentioned.

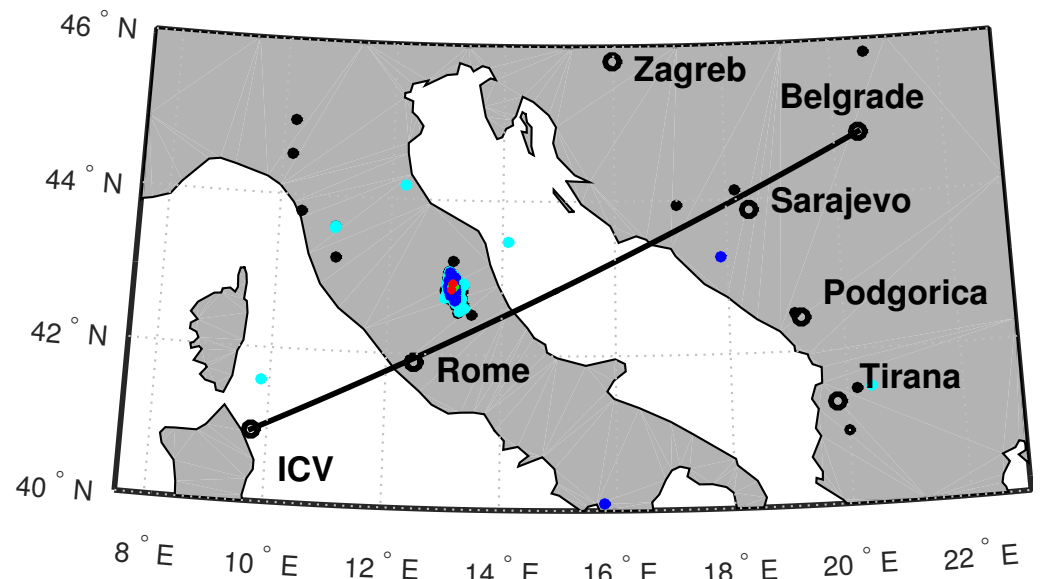


**Figure 2.** Map of the observed area around the path of the signal transmitted by the ICV transmitter located in Italy and received in Belgrade, Serbia. The epicentres of the earthquakes of magnitudes  $M < 3$ ,  $3 \leq M < 4$ ,  $4 \leq M < 5$ ,  $5 \leq M < 6$ , and  $M \geq 6$  that occurred in the period from 26 October to 2 November 2016 are represented by black, cyan, blue, green, and red dots, respectively.

**Table 1.** List of the considered earthquakes with magnitudes  $M \geq 4$ . Data for dates, times, epicentres (latitudes and longitudes), magnitudes, and the corresponding scale (the symbols Mw, mb, and ML denote the moment magnitude [33], body-wave magnitude [34] and Richter [35] scales, respectively) are given in [32].

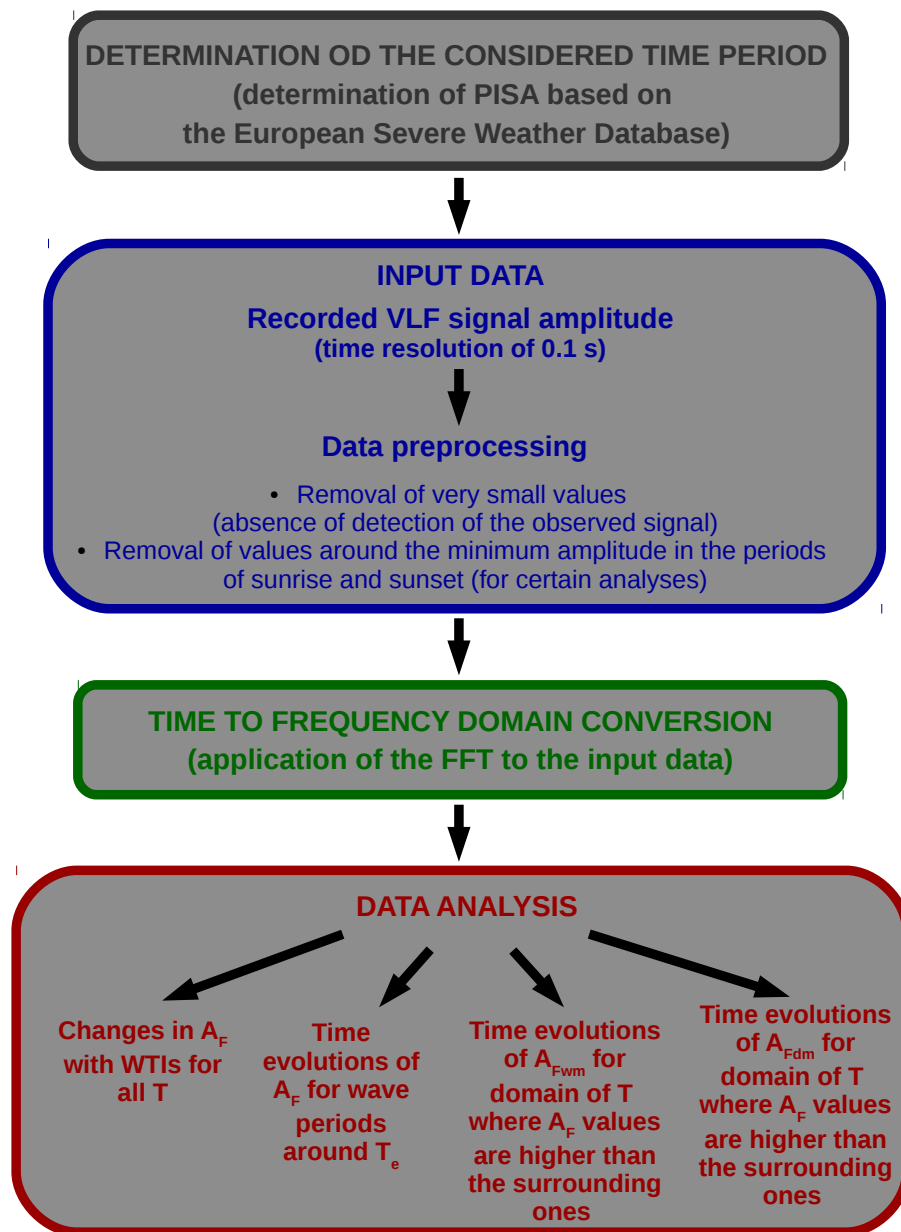
No	Date	Time (UT)	Latitude (°)	Latitude (°)	Magnitude
DAY 1					
1	26 October 2016	17:10:36	42.88	13.13	Mw 5.5
2	26 October 2016	19:16:57	42.88	13.16	ML 4.3
3	26 October 2016	19:18:07	42.92	13.13	Mw 6.1
4	26 October 2016	21:24:51	42.87	13.08	mb 4.1
5	26 October 2016	21:42:02	42.86	13.13	Mw 4.7
6	26 October 2016	23:52:32	42.82	13.14	mb 4.0
DAY 2					
7	27 October 2016	00:21:32	42.96	13.06	mb 4.2
8	27 October 2016	03:19:27	42.84	13.15	mb 4.4
9	27 October 2016	03:50:24	42.99	13.13	Mw 4.2
10	27 October 2016	08:21:46	42.87	13.10	Mw 4.4
11	27 October 2016	17:22:23	42.84	13.10	ML 4.2

Table 1. Cont.

No	Date	Time (UT)	Latitude (°)	Latitude (°)	Magnitude
DAY 3					
-					
DAY 4					
12	29 October 2016	11:58:07	40.09	15.79	ML 4.3
13	29 October 2016	16:24:33	42.81	13.10	mb 4.4
DAY 5					
14	30 October 2016	06:40:18	42.84	13.11	Mw 6.5
15	30 October 2016	06:55:40	42.74	13.17	ML 4.1
16	30 October 2016	07:00:40	42.88	13.05	ML 4.1
17	30 October 2016	07:05:56	42.79	13.16	ML 4.1
18	30 October 2016	07:13:06	42.73	13.16	ML 4.5
19	30 October 2016	07:07:54	42.70	13.17	mb 4.2
20	30 October 2016	07:34:47	42.92	13.13	ML 4.0
21	30 October 2016	08:35:58	42.83	13.08	mb 4.6
22	30 October 2016	10:19:26	42.82	13.14	ML 4.1
23	30 October 2016	11:21:09	43.06	13.08	ML 4.1
24	30 October 2016	11:58:17	42.84	13.06	ML 4.0
25	30 October 2016	12:07:00	42.84	13.08	ML 4.6
26	30 October 2016	13:34:54	42.80	13.17	ML 4.6
27	30 October 2016	18:21:09	42.79	13.15	ML 4.2
DAY 6					
28	31 October 2016	03:27:40	42.77	13.09	mb 4.3
29	31 October 2016	07:05:45	42.83	13.17	Mw 4.2
30	31 October 2016	09:38:13	43.26	17.88	ML 4.2
DAY 7					
31	1 November 2016	07:56:39	43.00	13.16	Mw 4.9
DAY 8					
32	2 November 2016	19:37:52	42.89	13.11	ML 4.0

### 3. Data Processing

The investigation of the excitations and attenuations of small-period waves by processing the amplitude of the VLF signal in this study is based on the procedures applied in previous relevant studies [27,28,30]. For this reason, we only list the main features of these procedures in this section. In addition, Figure 3 provides a flowchart that visually explains the processing steps.



**Figure 3.** A flowchart explaining the processing steps in this study: (a) determination of the considered time period using the Euro-Mediterranean Seismological Centre [32], (b) determination of the input VLF data and corresponding data preprocessing, (c) time- to frequency-domain conversion using the fast Fourier transform (FFT), and (d) data analysis. Data analysis relates to time dependencies of (i) the Fourier amplitude  $A_F$  for all values of wave periods  $T$ , (ii)  $A_F$  for wave periods around values of  $T_e$  for which wave excitations are visible around the time of earthquakes that occurred during PWISA, (iii) mean values  $A_{Fwm}$  of  $A_F$ , and (iv) daily mean values  $A_{Fdm}$  of  $A_{Fwm}$  in the window time intervals (WTIs) in the domain of  $T$  for which higher values are observed compared to the surrounding ones.

### 3.1. Input Data

The input data were the values of the ICV signal amplitude recorded by the AbsPAL receiver in Belgrade, Serbia. The time resolution of these data was 0.1 s.

Bearing in mind that not all values of the input data are relevant due to artificial influences (e.g., the signal was not broadcast in certain periods) or due to the dominant influence of other natural phenomena such as sunrise and sunset on their variations,

the data were preprocessed before the analysis in the frequency domain. It consisted in eliminating the data (i.e., replacing them with NaN values) recorded in the periods:

- In which the amplitude values were too low (this indicated the absence of ICV signal detection). This process was carried out for all shown analyses.
- Around the amplitude minima that are characteristic during sunrise and sunset. These data were only eliminated in cases where the increase in  $A_F$  was significant and only in determining the mean daily values of the considered parameters.

### 3.2. Frequency Domain

The analysis in the frequency domain is made possible by applying the FFT to the input data recorded in the time domain. As in previous studies, the FFT was applied to window time intervals (WTIs) of 20 min, 1 h, and 3 h. In this study, the WTIs were shifted by steps of:

- Ten minutes in all three cases in 3D representations of the  $A_F(T, t_{ws})$  dependence;
- Twenty minutes for analyses based on determining mean values in 20 min intervals (so all recorded data were included in the analysis, and due to the non-overlapping WTIs, a single value was included in the mean value representing only one WTI).

As in the mentioned earlier relevant studies, the Fourier amplitude  $A_F$  was represented as a function of the wave period  $T$ , which corresponds to the reciprocal value of the frequency  $f$  obtained directly by applying the FFT to the input data ( $T = 1/f$ ). A minimum value of  $T$  of 0.2 s was determined as twice the time resolution of the recorded data, and its maximum values depended on the observed WTIs and were half of their values, i.e., 10 min, 30 min, and 90 min.

We emphasise at this point that although we observe dependencies on  $T$ , we use the term “frequency domain” in this, as well as in previous relevant studies, because it is the most common term found in the relevant literature and because of the very simple and well-known relationship between these two physical quantities.

### 3.3. Data Analysis

The data analysis in this study can be divided into four parts:

- **Visualisation of the changes in  $A_F$  with WTIs which are represented by the times of their beginnings  $t_{ws}$  for all values of  $T$ .** The error in the determination of  $t_{ws}$  is equal to the time resolution of the recorded data (0.1 s). Bearing in mind that it is significantly smaller than the value of  $t_{ws}$ , it can be considered approximately negligible. This also applies to other analyses in which this parameter is used. In the case of an error in the determination of  $T$ , there are two cases that depend on the values of  $T$ . This explanation is given in [30] and is based on the fact that by applying the FFT to data recorded at equidistant time intervals, equidistant values of  $f$  are obtained. Given that  $T = 1/f$ , the distance between neighbouring values of  $T$  increases with it. The distance for small values of  $T$  can be calculated as  $\Delta T = \Delta f / f^2 = T^2 \Delta f$  where  $\Delta f = 1/\text{WTI}$  and has values of  $8.3333 \times 10^{-4}$  Hz,  $2.7778 \times 10^{-4}$  Hz, and  $9.2593 \times 10^{-5}$  Hz for WTIs of 20 min, 1 h, and 3 h, respectively. The error for the higher periods is determined by the absolute difference between a certain value of  $T$  and the first larger discrete value of this parameter. In this study, only a visual analysis was performed for higher values of  $T$ , so that error was only determined in the first way.
- **Analysis of  $A_F$  in WTIs starting at  $t_{ws}$  for wave periods around values of  $T_e$  for which wave excitations are visible around the time of earthquakes that occurred during PWISA.** We performed analyses for all values of  $T_e$  that are specified in [30]: 0.2000 s, 0.2333 s, 0.3500 s, 0.4677 s, 0.7001 s, and 1.400 s. In order to take into account the possibility of more significant changes in very close periods, we considered the maximum value  $A_F^*$  of  $A_F$  values for the considered  $T_e$  and for 5 of its closest larger and smaller values in WTI starting at  $t_{ws}$ :

$$A_F^*(t_{ws}) = \max\{A_F^*(T_e(i_e - 5 : i_e + 5), t_{ws})\}, \quad (1)$$

where  $i_e$  is the ordinal position assigned to the element that represents  $T_e$  in the data array for  $T$ . Taking into account the analysis of the error in the determination of  $T$  in the previous point and the fact that this analysis is relevant for WTI = 20 min, it can be approximately assumed that in this case,  $\Delta T_e = 5 \times 8.3333e^{-4} T_e^2$  s, where  $T_e$  is expressed in s.

- **Analysis of the mean values  $A_{Fwm}$  of  $A_F$  in WTIs starting at  $t_{ws}$  in the domain of  $T$  for which higher values are observed compared to the surrounding ones.** This parameter was calculated as follows:

$$A_{Fwm}(t_{ws}) = \frac{\sum_{i=1}^N A_F(i, t_{ws})}{N}, \quad (2)$$

where  $N$  is the total number of  $A_F$  values in the considered WTI for the chosen  $T$  domain, and  $i$  is the ordinal position of a particular value in this array.

- **Analysis of the time evolution of daily averaged values  $A_{Fdm}$  of  $A_{Fwm}$  in the domain of  $T$  for which higher values are observed compared to the surrounding ones.** This parameter was calculated by the following expression:

$$A_{Fdm} = \frac{\sum_{j=1}^D A_F(j)}{D}, \quad (3)$$

where  $D$  is the total number of relevant  $A_F$  values in the considered day, and  $j$  is the ordinal position of a particular value in this array. We emphasise here that incorrect data were not considered in the respective analyses, so that  $D$  was not the same for all days. The analyses were performed both for its absolute values in the considered  $T$  domain and for its corresponding relative values  $r$  in relation to the reference domain with Fourier amplitude  $A_{Fdm}^{ref}$ :

$$r = \frac{A_{Fdm}}{A_{Fdm}^{ref}}. \quad (4)$$

In this way, we analysed the localisation of the observed differences, which is significant because, as seen in Section 4, in some cases, it is clearly visible, while in others, it is not. From this, we can conclude that the corresponding changes in the value of  $A_F$  over time have different causes.

The time evolutions of the mentioned parameters related to  $A_F$  were also compared with the corresponding time evolutions of the relevant noise amplitude (denoted as  $A_{noise}$  when referring to a particular WTI, and  $A_{noisedm} = \sum_{j=1}^D A_{noise}(j)/D$  when referring to a particular day). The determination of  $A_{noise}$  is explained in detail in [36] and used in [30] and the relevant references therein.

#### 4. Results and Discussion

The investigation of the ICV signal amplitude changes in the frequency domain, which can possibly be linked to processes in the lithosphere during the PISA in Central Italy from 26 October to 2 November 2016, was carried out in two phases. To distinguish the periodic changes that occurred during the day, we first performed an analysis for a quiet period (Section 4.1). Then, we studied the results of the FFT application on the signal amplitude values recorded on the analysed days. In these analyses,  $A_F$  and the corresponding parameters are shown (a) for whole days, for all values of  $T$  (the dependences  $A_F(T, t_{ws})$  are shown in 3D graphs), for the selected values around  $T_e$  for which wave excitations were observed in the periods around the considered earthquakes that occurred during PIWSA [30] (we present time evolutions of  $A_F^*$  and  $A_{Fwm}$ ), and (b) for a one-month period that included the eight-day period as well as the periods before and after (we present time evolutions of  $A_{Fdm}$ ).

In the presented analyses, we excluded the intervals in which the recorded amplitude values were visibly disturbed by unnatural influences (e.g., the time periods in which no signal was emitted). In the analyses covering a period of one month, we also omitted the intervals during sunrises and sunsets in which the amplitude noise was increased. In this way, the influence of these factors on the analyses in the frequency domain was avoided, which is important as they are not always clearly visible on the presented graphs.

#### 4.1. Quiet Conditions

In this analysis, the determination of the characteristics of the considered VLF signal under quiet conditions was complex. Namely, the seismic activity in Central Italy was intensified over a long time period. Therefore, it was not possible to single out an entire day immediately before or after the eight-day interval analysed in this study during which there were no earthquakes. For this reason, the analysis of the reference periods which are intended to show the periodic changes in  $A_F$  was carried out for two days:

- On 3 October 2010, when the conditions were quiet and not a single earthquake was recorded.
- On 25 October 2016 (the day before the analysed period), during which the amplitude noise was stable with values around 2 dB except for a short period during the afternoon when an earthquake of magnitude ML 3.9 occurred in Central Italy [29].

It is important to emphasise here that both selected days were in October, as was the beginning of the observed eight-day period. In this way, possible seasonal variations in the amplitude characteristics in the frequency domain were avoided.

##### 4.1.1. First Reference Day: 3 October 2010

The dependence  $A_F(T, t_{ws})$  during 3 October 2010 is shown in Figure 4.

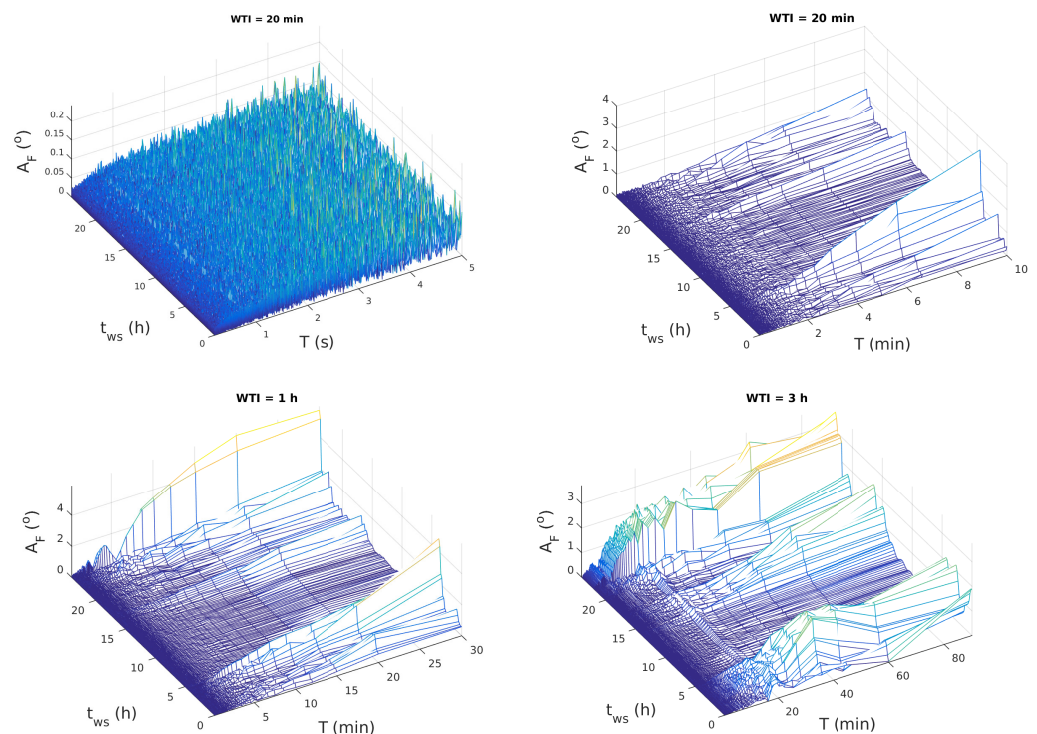


**Figure 4.** Fourier amplitude  $A_F$  of waves with period  $T$  obtained by applying the FFT to the ICV signal amplitude recorded on 3 October 2010 with window time intervals (WTIs) of 20 min (**upper panels**), 1 h (**bottom left panel**), and 3 h (**bottom right panel**) starting at  $t_{ws}$ .

In the upper left panel, which shows the time evolution of  $A_F$  (obtained by applying the FFT to data in WTIs of 20 min) up to  $T = 5$  s, no significant changes can be seen. In other words, the potential changes in these domains cannot be periodic daily changes. In the other three panels (upper left panel for WTI = 20 min, and lower left (WTI = 1 h) and right (WTI = 3 h) panels), periodic changes are visible for  $T$  greater than about 2 min. They are manifested by increases in the  $A_F$  values during the sunrise and sunset periods with the highest values before 5 UT as well as after 15 UT and towards the end of a day.

The lack of changes for  $T \leq 5$  s is consistent with the results in the quiet period from 19:00 UT on 3 November 2009 to 4:00 UT on 4 November 2009 [30]. Moreover, the mentioned variations for  $T$  longer than a few minutes are consistent with those obtained in the corresponding analyses related to the time periods around the analysed earthquake near Kraljevo (3 November 2010) [27] and the earthquakes near Kraljevo (4 November), in the Tyrrhenian Sea and in the Western Mediterranean Sea [30]. We emphasise here that although these are periods in which earthquakes with a magnitude greater than four occurred, no additional changes due to seismic activity were observed for the mentioned wave periods.

#### 4.1.2. Second Reference Day: 25 October 2016

The dependencies of  $A_F(T, t_{ws})$  during 25 October 2016 are shown in Figure 5. Comparing the obtained graphs with the corresponding ones from the previous figure, it can be noticed that the descriptions of the observed variations are very similar, except for the reduction in  $A_F$  in the afternoon, when the noise amplitude is also reduced (as already mentioned, this reduction can be associated with an earthquake in Central Italy). The only significant difference is the higher  $A_F$  values in the  $T$  domain between about 1.4 s and 2 s compared to the values for the other  $T$  values during the day.

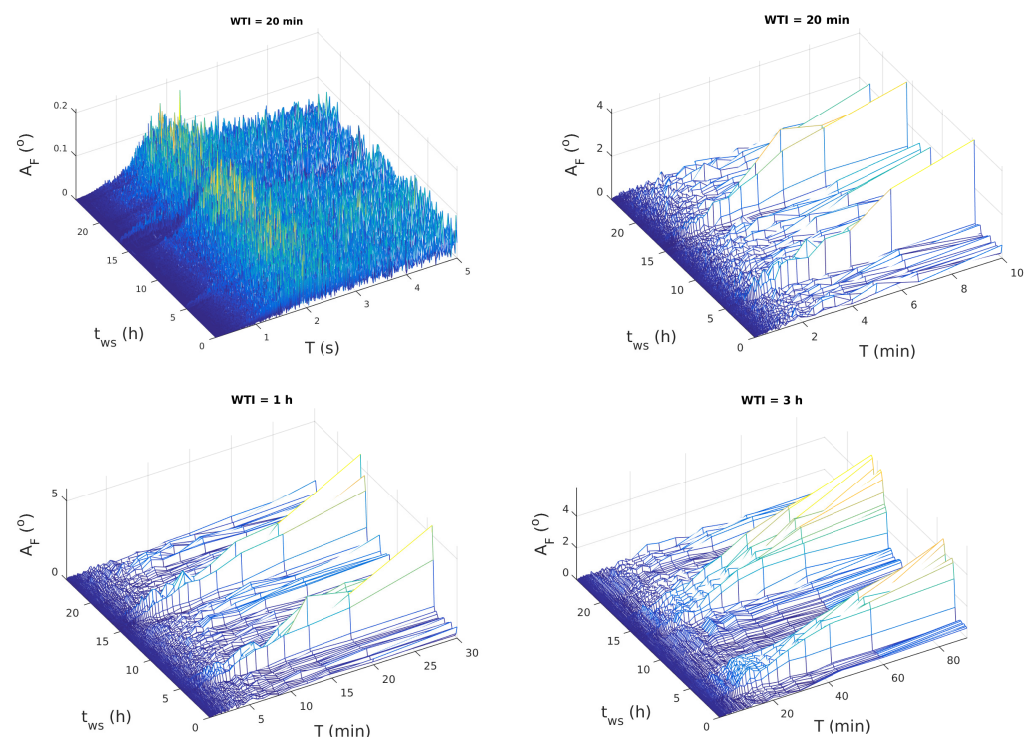


**Figure 5.** Fourier amplitude  $A_F$  of waves with period  $T$  obtained by applying the FFT to the ICV signal amplitude recorded on 25 November 2016 with window time intervals (WTIs) of 20 min (**upper panels**), 1 h (**bottom left panel**), and 3 h (**bottom right panel**) starting at  $t_{ws}$ .

#### 4.1.3. Comparisons of the Time Evolutions of $A_F$ for Narrow Domains of $T$ during the Observed Reference Days

In previous analyses of earthquakes that occurred during PWISA, wave excitations were observed at discrete  $T_e$  values. In addition, higher values of  $A_F$  were observed in the domain of  $T$  values between 1.4 s and 2 s on the second reference day (Section 4.1.2). To analyse the expected values of  $A_F$  under quiet conditions for these specific  $T$ , we compared their time evolutions for the considered two days, and their shapes with those of the amplitude noise  $A_{\text{noise}}$  during the corresponding time periods. The following parameters are shown in Figure 6:

- Upper panels: Maximum  $A_F$  values for each  $t_{\text{ws}}$  for six sets of 11 discrete  $T$  values determined around the values 0.2000 s, 0.2333 s, 0.3500 s, 0.4677 s, 0.7001 s, and 1.400 s, respectively (these values and their five closest lower and higher values). Based on the explanation in Section 3,  $\Delta T$  s for the given  $T$  in these analyses are 0.0002 s, 0.0003 s, 0.0006 s, 0.001 s, 0.003 s, and 0.009 s, respectively.
- Middle panels: mean  $A_F$  values for  $T$  between 1.4 s to 2 s for each  $t_{\text{ws}}$ .
- Bottom panels: the time evolutions of  $A_{\text{noise}}$  given in [29].

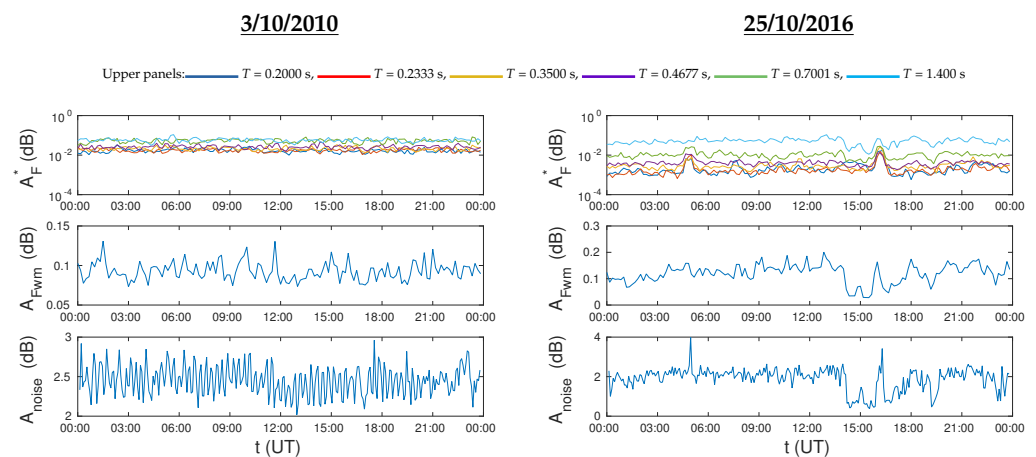


**Figure 6.** Time evolutions of the maximum values of the Fourier amplitude  $A_F^*$  for the observed wave periods  $T_e$  and the five closest high and low values (**upper panels**), the mean values of the Fourier amplitude  $A_{Fwm}$  for the wave periods  $T$  in the domain 1.4–2 s (**middle panels**), and the amplitude noise  $A_{\text{noise}}$  (**bottom panels**) in each window time interval (WTI) starting at  $t_{\text{ws}}$  for the reference days 3 October 2010 (**left panels**) and 25 October 2016 (**right panels**).

In the upper left panel, it can be seen that all displayed dependencies for the first reference day vary around very similar values throughout the day. This indicates that there is no significant influence of solar radiation and its changes on the observed values of  $A_F^*$ ,  $A_{Fwm}$  and  $A_{\text{noise}}$ . In this case, all values of  $A_F^*$  are approximately within one order of magnitude. Comparing the values of  $A_{\text{noise}}$  in the lower panels shows that its value is slightly lower for the second reference day. A more significant difference for the two observed days is visible in the upper panels. Namely, during the second day, a decrease in  $A_F^*$  is visible for all  $T_e$  except for  $T_e = 1.4$  s. This difference increases with a decrease in  $T_e$  and is more than 10 times greater for  $T_e = 0.2$  s. In the case of  $A_{Fwm}$ , higher values are observed for the second reference day. In other words, these comparisons for a quiet day outside the PISA and quiet parts of a day just before the PISA show a decrease in  $A_F$  values for the considered  $T < 1$  s and their increase for the  $T$  domain from 1.4 s to 2 s for the second considered day.

In the analysis of the second day, it is interesting to note that the reduction in  $A_{\text{noise}}$  in the afternoon is followed by a decrease in  $A_F^*$  for all observed values of  $T_e$ , except for its lowest value (0.2 s) where an increase in  $A_F^*$  is observed (this corresponds to the wave excitation at this wave period). This is important to emphasise because this reduction in

the amplitude noise can be related to the earthquake that occurred during its duration. However, the wave excitation at this  $T_e$  in periods around earthquakes that occurred during PWISA were only registered for one event in the amplitude and phase analyses, which is why they could not be associated with seismic activity based on previous analyses.

In addition, it can be seen that the effects of sunrise and sunset during the second reference day, which are seen as peaks in the time evolution of  $A_{\text{noise}}$ , cause increases in  $A_F^*$  for lower values of  $T_e$ , while no pronounced changes are seen for the highest observed  $T_e$  and for the domain of  $T$  from 1.4 s to 2 s.

#### 4.2. Seismic Active Period

As in previous relevant studies [27,28,30] and in Section 4.1, the analysis of ICV signal amplitude characteristics in the frequency domain was performed by applying the FFT to data sets recorded with a time resolution of 0.1 s, and to WTIs of 20 min, 1 h, and 3 h. The time evolutions of the processed signal amplitude during the observed days (from 26 October to 2 November 2016) are given in [29].

Bearing in mind that each displayed data point refers to the entire considered WTI, the accuracy of determining the time of occurrence of changes depends on its duration, and it was the best for WTI = 20 min and worst for WTI = 3 h. For this reason and due to the fact that the maximum relevant values of  $T$  are equal to half of the time interval to which the FFT is applied, the analysis of the changes was performed separately for three domains of  $T$ . These domains were between 0.2 s and 10 min (small wave periods), 10 min and 30 min (medium wave periods), and 30 min and 90 min (large wave periods), where  $A_F$  was obtained by applying the FFT to WTIs of 20 min, 1 h, and 3 h, respectively.

In the following analyses, the incorrect values were discarded as follows:

- The data in the period 9:00 UT–12:20 UT on 31 October were not processed in all analyses, as no ICV signal was detected in that period. This can be seen from the time evolution of its amplitude which is shown in [29]. For the same reason, the data from parts of several days that were considered for examining the beginnings and ends of multi-day changes were removed.
- In the case of an increased  $A_F$ , the recorded data in the periods of sunrise and sunset were not taken into account in the analyses of the daily values of  $A_{Fwm}$  and  $A_{\text{noise}}$ .

In this way, the influence of changes in the signal characteristics due to clearly visible artificial influences and other phenomena that occurred at sunrise and sunset was avoided. In the time periods relevant to the second case,  $A_F$  was displayed in 3D graphics to visualise the effects of changes in incident radiation in the morning and evening. This is also interesting because in previous studies, no differences were visible for small values of  $T$  in these periods of the day compared to others.

##### 4.2.1. Small Wave Periods

Based on the results of previous studies and the changes presented in Section 4.1, it can be concluded that analysing wave changes in the small-wave-period domain is the most important. In this domain, we analysed the following:

- The existence of wave excitations at  $T_e$  of 0.2333 s, 0.3500 s, 0.4677 s, 0.7001 s, and 1.400 s, which were visible in the cases of the previously analysed earthquakes that occurred during PWISA;
- Values of  $A_{Fwm}$  for the domain  $T$  from 1.4 s to 2 s, which were higher than other close values of  $T$  on almost all days from 26 October to 1 November;
- Attenuations of the waves at low wave periods.

**Analyses of 3D graphs:** The 3D graphs obtained by applying the FFT to the WTI of 20 min are shown in Figure 7 in two parts for each day, as the  $A_F$  values for lower and higher values of  $T$  were very different. The threshold value was  $T = 5$  s. Low values are shown on the left, and higher values on the right.

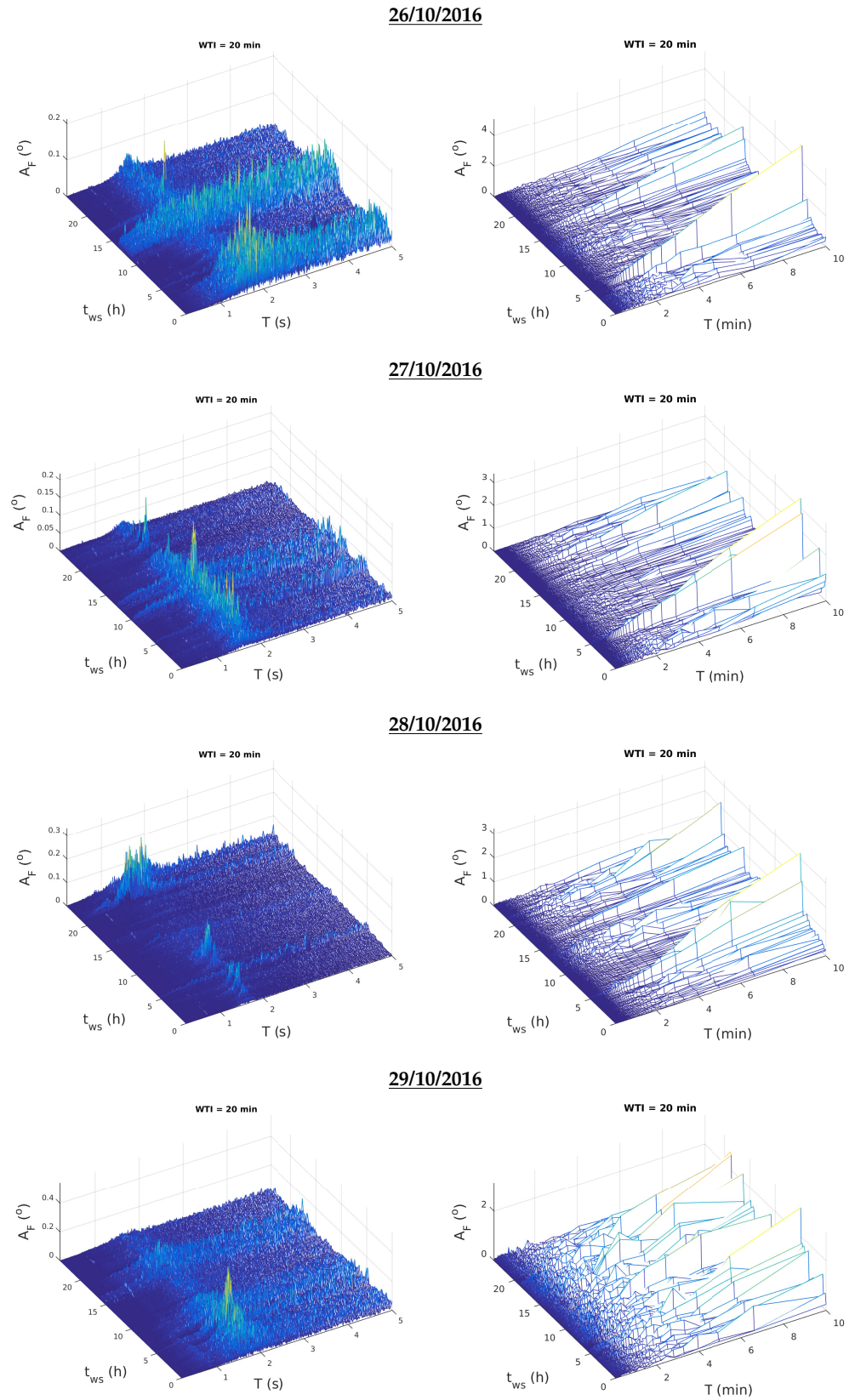
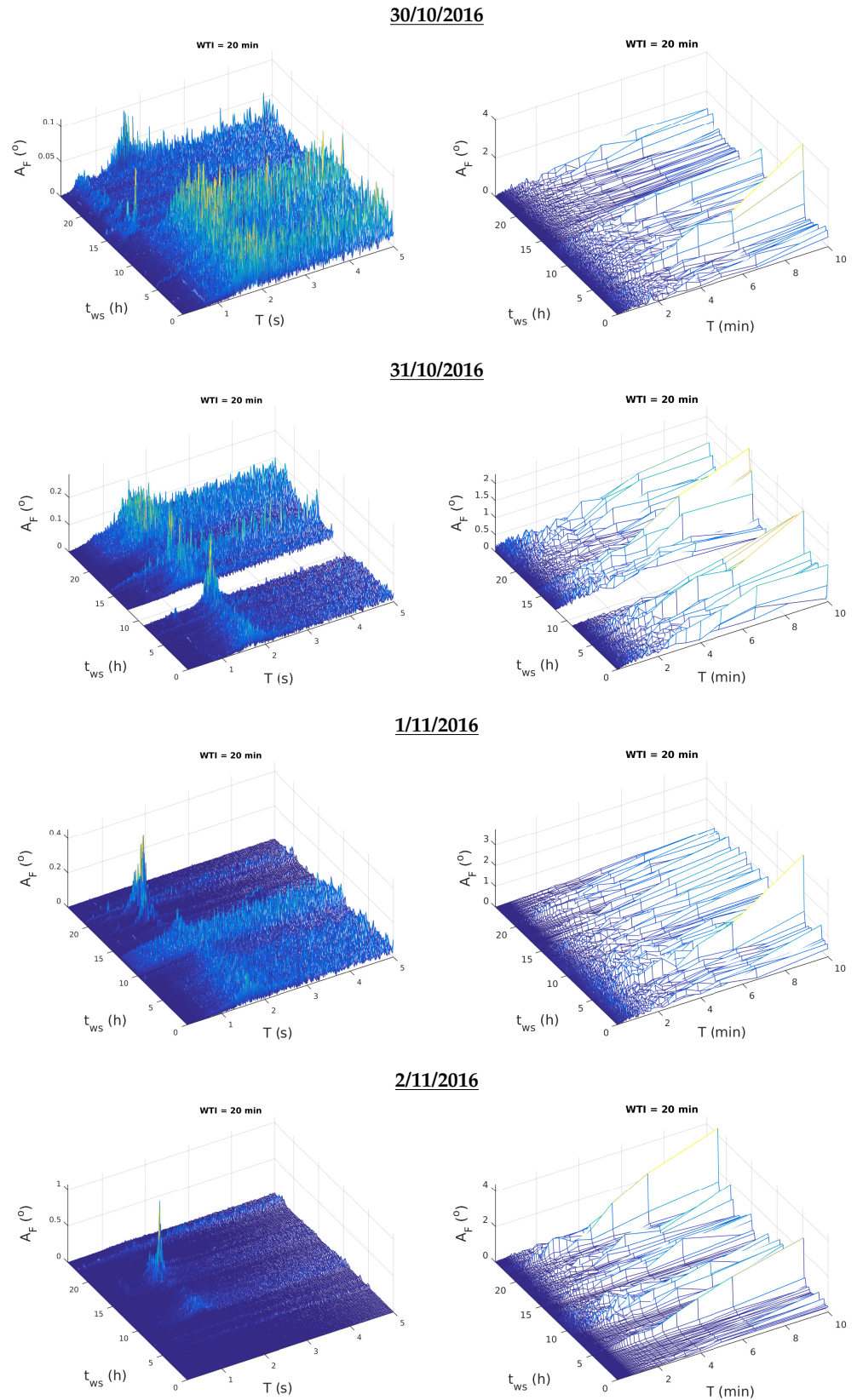


Figure 7. Cont.



**Figure 7.** Dependencies of the Fourier amplitude  $A_F$  on the wave period  $T$  and the start time  $t_{ws}$  of the window time intervals (WTIs) from 26 October to 2 November 2016. The results of applying the fast Fourier transform to the WTI of 20 min for  $T \leq 5$  s and  $T > 5$  s are shown in the left and right panels, respectively.

Before analysing the wave excitations and attenuations, it is important to note the following changes compared to the results of the analyses of the reference days in Section 4.1 and the studies presented in [27,30]:

- With the exception of time intervals of a few hours on 26, 29, and 31 October and on 1 November, the  $A_F$  values for  $2 \text{ s} < T \leq 5 \text{ s}$  were significantly lower than the values given for the reference days in Figures 4 and 5. During the isolated intervals,  $A_{\text{noise}}$  was approximately equal to the values recorded on quiet days (see [29] and Figure 8).
- Although it is not noticeable on the 3D graphs due to the significantly smaller values of  $A_F$  compared to their maximum, the values of this parameter for a small  $T$  were about an order of magnitude smaller than the values recorded on the first reference day (3 October 2010), which was also true for the values recorded on 25 October 2016 (the second reference day). This can be clearly seen in Figure 8.
- When the  $A_F$  values were small in the periods of sunrise and sunset, smaller increases in  $A_F$  were observed for  $T \leq 5 \text{ s}$  in the short term.

From the 3D graphs presented in Figure 7, it can be seen that there are no long-term pronounced increases in  $A_F$  at discrete values of  $T$ , including those for which wave excitations with onset prior to the observed earthquakes were visible in previous studies. Although short increases in  $A_F$  compared to its surrounding values were observed on all days, the obtained values were lower than those observed on quiet days.

Higher values of  $A_F$  in the domain of  $T$  from 1.4 s to 2 s compared to the others for  $T < 5 \text{ s}$  were observed on all days from 26 October to 1 November with shorter interruptions on 26, 27, and 30 October. However, these higher values were only approximately comparable to those obtained on quiet days, except in short-term periods when significant increases were visible. These increases were observed on all days except 30 October and are analysed in more detail in the description of Figure 8.

On the last observed day, the  $A_F$  values were very low throughout the day, with the exception of shorter intervals for the isolated domain  $T$  (around 9 UT and 17 UT). In the second case,  $A_F$  reached the highest values in the observed eight-day interval (about 1 dB).

In addition to the mentioned variations, a shift of higher  $A_F$  values from the mentioned domain to the domain of  $T$  values from about 0.4 s to about 1 s was observed. In the observed time interval, this change was only registered on 30 October. The largest number of earthquake occurred on that day (268, see Figure 1). However, they occurred throughout the day and it is not possible to establish a connection between the aforementioned changes and the occurrence of an earthquake. On the other hand, the time evolutions of the signal amplitude and its noise indicated a sharp decrease in the value of both these signal parameters (amplitude noise reduction of Type 3) in the period of the shift of higher  $A_F$  values to smaller wave periods. The ends of the mentioned changes in all three parameters were towards the end of that day when the higher values of  $A_F$  returned to the original domain of  $T$  with higher values.

The comparison of time evolutions of  $A_F$  for small wave periods for  $T > 5 \text{ s}$  (right panels in Figure 7) with corresponding graphs for reference days (upper right panels in Figures 4 and 5) shows that there are no significant changes that can be associated with the PISA. Namely, the largest increases in  $A_F$  for these values of  $T$  were before 5 UT, after 15 UT, and toward the end of a day or around midnight, which was already registered during the two observed days in Section 4.1. The only changes could be observed on 1 November, when the latter two mentioned increases were not observed due to lower values of  $A_F$  in that period of the day than in other cases, but they could not be associated with seismic activity.

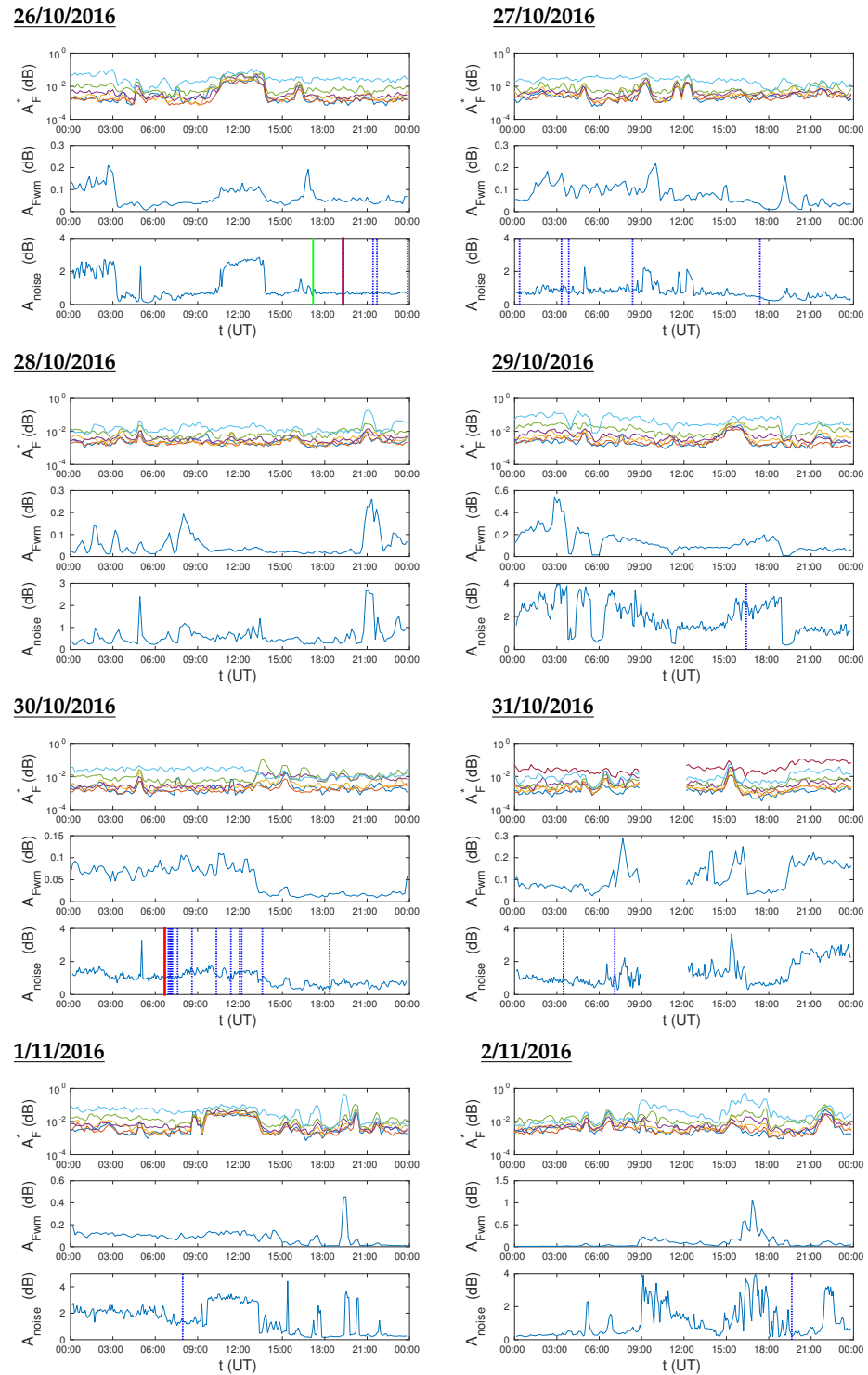


**Figure 8.** Time evolutions of the maximum values of the Fourier amplitude  $A_F^*$  for the observed wave periods  $T_e$  and the five closest higher and lower values (**upper panels**), the mean values of the Fourier amplitude  $A_{Fwm}$  for the wave periods  $T$  in the domain 1.4–2 s (**middle panels**), and the amplitude noise  $A_{noise}$  (**bottom panels**) in each window time interval (WTI) starting at  $t_{ws}$  for the period from 26 October to 3 November 2016. The shown blue, green, and red vertical lines indicate the times of the earthquakes with magnitudes between 4 and 5, between 5 and 6, and greater than 6, respectively.

**Analyses of  $A_F^*$  for the wave periods  $T_e$  and  $A_{F_{wm}}$  between 1.4 s and 2 s.** To visualise and compare the described changes in the Fourier amplitude more clearly and to compare the changes in the frequency and time domains, we show the relevant dependencies in Figure 8. The time evolutions of  $A_F^*$  for  $T_e$  and the mean values  $A_{F_{wm}}$  of  $A_F$  for  $T$  in the domain 1.4–2 s are presented in the upper and middle panels, respectively. The time evolution of  $A_{noise}$  is given in the lower panels, where the times of the earthquakes in Central Italy given in Table 1 are marked with vertical lines. The values for  $A_F^*$  and  $A_{F_{wm}}$  are determined using the procedure explained in Section 3, while the procedure for the determination of  $A_{noise}$  is developed in [36] and explained in earlier studies (see [30] and references therein).

As one can see in the middle panels of Figure 8, significant short-term increases in the  $A_{F_{wm}}$  values were observed on all days except 30 October. Their maxima were sometimes preceded by the maxima of  $A_F^*$  at all  $T_e$  (except in some cases for its maximum value). However, due to the occurrence during the larger values of  $A_{noise}$  and due to the end before the shown times of stronger earthquakes, these wave excitations had different characteristics than those recorded in previous studies at  $T_e$  (they lasted throughout the reduction in the signal amplitude noise and end after the considered earthquake). Moreover, there was no regularity in their occurrence with respect to the occurrence of stronger earthquakes, which is why they are probably the consequence of other phenomena.

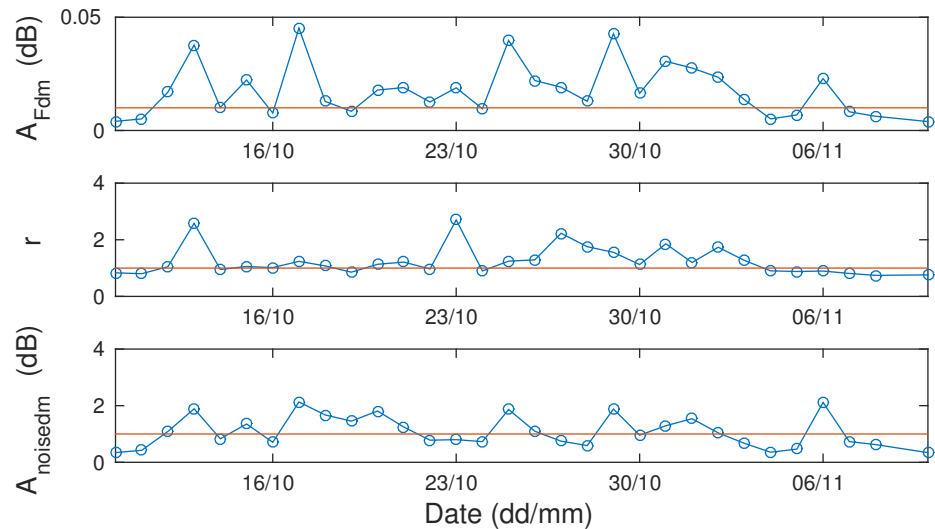
The analysis of the shapes of the displayed dependencies indicated that there were no wave excitations at low periods  $T_e$  and in the observed domain  $T$  from 0.4 s to 2 s in the periods around the stronger shown earthquakes. At the same time, it can be seen that these shapes were more similar to the shape of the time evolution of  $A_{noise}$ . In addition, if we compare their values with the relevant values obtained for the reference days, we can conclude that they are more similar to the reference day that preceded the observed PISA. This is very important because it opens the question of whether the PISA can be predicted on the basis of these parameters (or whether long-term seismic activity can be expected after the first strong earthquake). This possibility should be examined in the analyses of the beginnings of a statistically significant number of PISAs.

**Long-term analysis of  $A_{F_{dm}}$  for  $T$  between 1.4 s and 2 s.** As already mentioned, seismic activity was present in Central Italy before and after the observed PISA. In addition, the analysis of the amplitude noise in [29] in October 2016 (end of 24 October) showed that its values were below 2 dB, which differed from the expected state in quiet conditions. Only two multi-hour periods were observed in this interval (approximately from 3 UT to 8 UT on 13 October and from 6 UT to 11 UT on 15 October), which can be provisionally considered as quiet periods.

In this study, we investigated the daily mean values of  $A_{F_{wm}}$  in the  $T$  domain from 1.4 s to 2 s, denoted as  $A_{F_{dm}}$ , in a one-month time interval from 10 October to 10 November 2016. In addition to analysing the absolute values of this parameter, we give their ratio ( $r = A_{F_{dm}} / A_{F_{dm}}^{ref}$ ) to the corresponding values of  $A_{F_{dm}}^{ref}$  in the reference domain  $T$ , which was taken from 2.4 s to 3 s (no deviations in  $A_F$  in this domain from the corresponding values for the surrounding values of  $T$  were recorded). The obtained results are shown in Figure 9, where the bottom panel shows the daily mean averaged values of the amplitude noise (this time evolution was added to compare the changes in the time and frequency domains). In contrast to the analysis in [29], all shown values were determined only for intervals in which their values were not influenced by other known factors (see Section 4).

In the upper panel of this figure, the variations in  $A_{F_{dm}}$  with the maximum value of 0.4517 dB (17 October) can be seen. Bearing in mind that the corresponding value for 3 October 2010 and the first half of 25 October 2016 (when no earthquakes were recorded) were 0.0929 dB and 0.1236 dB, respectively, it can be concluded that  $A_{F_{dm}}$  was smaller than the expected values during quiet conditions in the entire considered period. The smallest values were found at the beginning and at the end of the observed interval, when larger relevant values were obtained for the reference  $T$  domain (seen in the middle panel ( $r < 1$ )). The peak values were visible throughout the entire observed interval, so they could not

be associated with the PISA. On the other hand, higher values of  $A_{Fdm}$  were obtained in relation to  $A_{Fwm}^{ref}$  during the entire considered PISA (more significant deviations were obtained on 6 out of 8 days), which was not the case in the periods before and after. Namely, the relevant increase was only visible on 13 and 23 October, while the considered values were similar for other days ( $r$  was approximately one). If we compare the upper and middle panels with the bottom one where the values of  $A_{noisedm}$  are given, we can see similar shapes of the changes in  $A_{Fdm}$  in the frequency domain with the specified parameter in the time domain. Looking at the variations in  $r$ , it can be concluded that the changes in the time domain are more visible at the lower observed values of  $T$ .

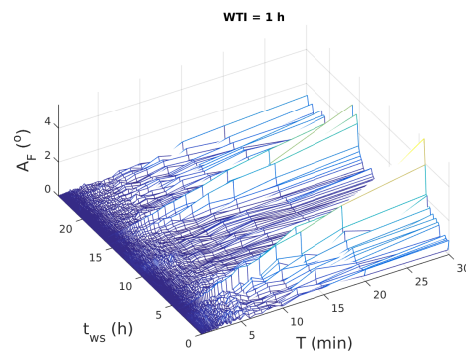
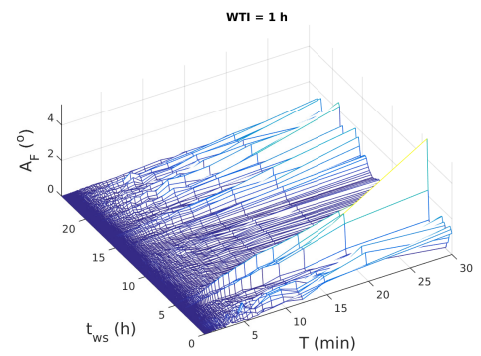
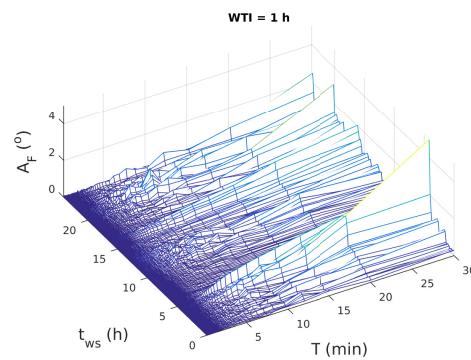
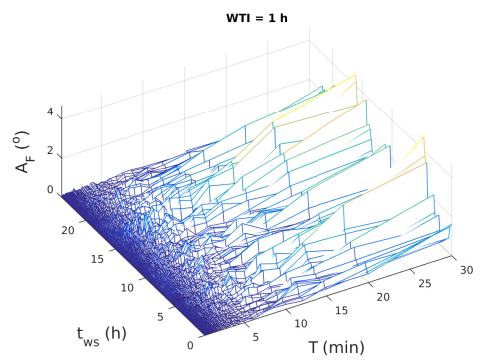
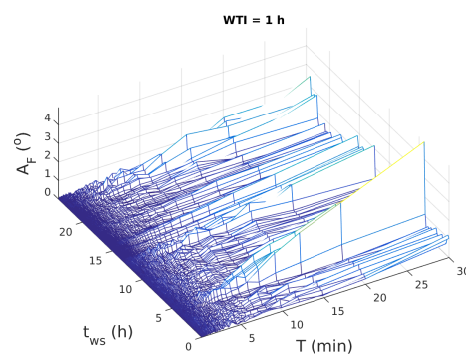
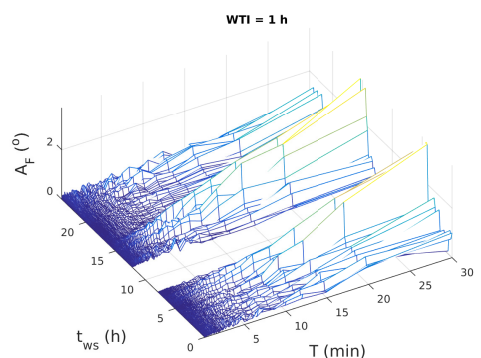
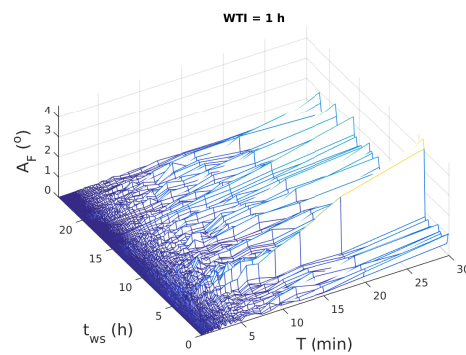
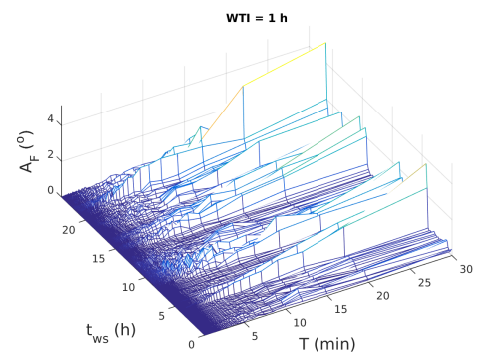


**Figure 9.** Time evolutions of the daily average values of  $A_{Fwm}$  in the  $T$  domain from 1.4 s to 2 s, denoted as  $A_{Fdm}$  (**upper panel**), its ratio ( $r$ ) to the corresponding values of  $A_{Fwm}^{ref}$  in the reference domain  $T$ , ranging from 2.4 s to 3 s (**middle panel**), and the daily mean amplitude noise  $A_{noisedm}$  (**bottom panel**) for the period from 10 October to 10 November 2016.

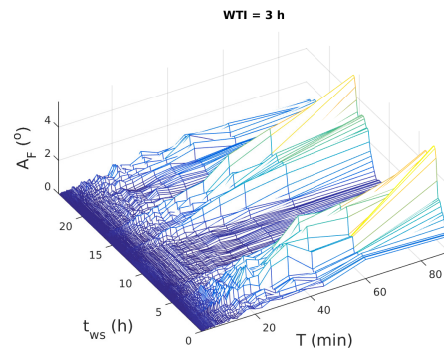
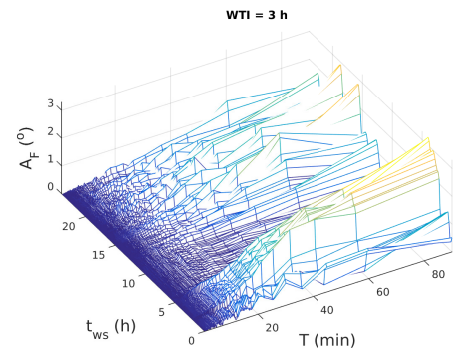
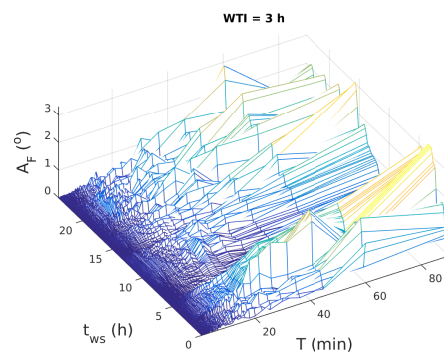
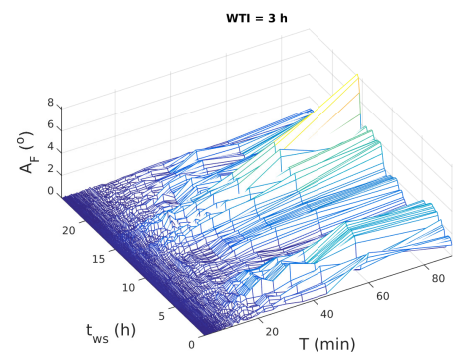
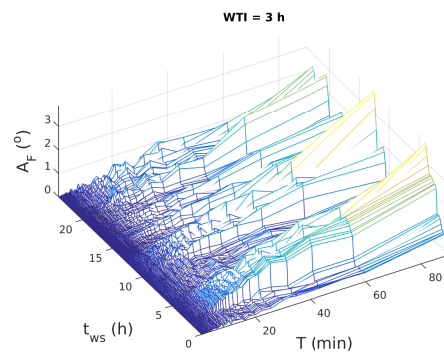
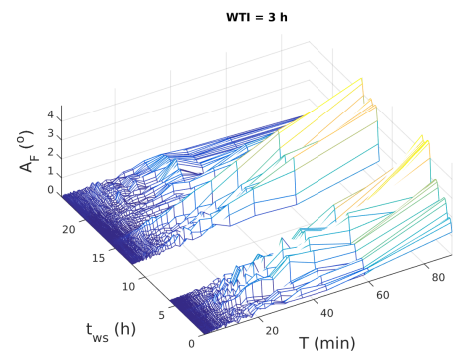
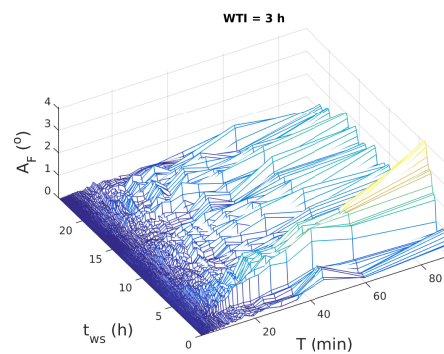
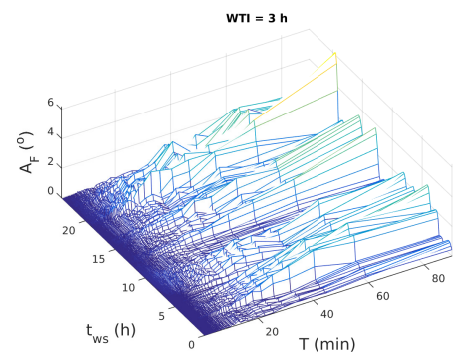
The mentioned changes before and during the PISA are potential precursors of this period in the frequency domain. Their differences from the changes recorded before the earthquake during PWISA are very significant as they can indicate long-term earthquake hazards. As in previous relevant studies, these assumptions should be tested in statistical analyses. Analysing other independent data is also necessary to explain the detected changes. Namely, VLF signals spread between transmitters and receivers located several hundred or thousand kilometres apart in the Earth-ionosphere waveguide, which is over 70 km high during the daytime and over 80 km high during the nighttime. As the amplitude and phase values recorded by a receiver provide information about the integral changes of a signal in this entire space, it is not possible to spatially localise the cause of the detected changes using these measurements alone.

#### 4.2.2. Medium and Large Wave Periods

To analyse medium (10–30 min) and long (30–90 min) wave periods, we used the results of the FFT application on WTIs of 1 h and 3 h, which are shown in Figures 10 and 11. The conclusions from comparing these graphs with the corresponding graphs in Figures 4 and 5 are the same as those mentioned in Section 4.2.1 for  $5 \text{ s} < T \leq 10 \text{ min}$ . In other words, no changes that can be associated with seismic activity were observed in these  $T$  domains compared to the reference days.

**26/10/2016****27/10/2016****28/10/2016****29/10/2016****30/10/2016****31/10/2016****1/11/2016****2/11/2016**

**Figure 10.** Dependencies of the Fourier amplitude  $A_F$  on the wave period  $T$  and the start time  $t_{ws}$  of the window time intervals (WTIs) of 1 h from 26 October to 2 November 2016.

26/10/201627/10/201628/10/201629/10/201630/10/201631/10/20161/11/20162/11/2016

**Figure 11.** Dependencies of the Fourier amplitude  $A_F$  on the wave period  $T$  and the start time  $t_{ws}$  of the window time intervals (WTIs) of 3 h from 26 October to 2 November 2016.

We point out here that the upper limit of  $T$  of the domain in which  $A_F$  values are lower than expected in a quiet period is several minutes or in the domain of medium wave periods. Its exact determination is not possible due to the long time period of the aforementioned reduction and variability in  $A_F$ , and also due to the fact that the determination of this parameter is approximately possible even for short time intervals of a few dozens of minutes.

#### *4.3. Analysis of the Reliability of the Relationship between Recorded Signal Changes and Seismic Activity and Possible Influences of Other Phenomena*

Changes in VLF signals used to monitor the ionosphere can be the result of numerous influences from processes and phenomena both from space and from the Earth's layers. They relate to meteorological and geomagnetic conditions (influences of changes in the atmosphere on VLF signals are shown in numerous papers, see, e.g., [37] and references therein), as well as to extraterrestrial radiation (changes in the VLF signal are most strongly influenced by solar X-ray flares [38–43], and the possibility of a multi-hour influence of gamma ray bursts on these signals has also been confirmed [44]).

In some cases, changes in VLF signals caused by different phenomena have the same or very similar characteristics. In addition, the detection of some phenomena depends on a large number of parameters, leading to differences in their characteristics. Therefore, statistical studies are necessary to confirm certain correlations. In the case of earthquakes, this confirmation is very complex because the perturbations are local, and there are numerous parameters that can influence detection. They relate to:

- Earthquake characteristics (characteristics of the location where it occurred, the depth at which it occurred, its magnitude);
- The occurrence of other earthquakes (near the epicentre of the observed earthquake or at distant locations that are also near the propagation path of the observed signal) and their characteristics;
- The epicentre position in relation to the propagation path of the observed signal (their mutual distance, the epicentre position in relation to the considered transmitter and receiver);
- The state of the atmosphere during the analysed period;
- Characteristics of the observed signal, including parameters relevant to the observed transmitters and receivers.

For these reasons, research into the relationship between changes in the VLF signal and seismic activity should be divided into the following phases:

- Phase I: diagnostics of changes that can be regarded as potential precursor of an earthquake given the defined characteristics of the recorded parameters.
- Phase II: determining the parameters that characterise these changes based on the smaller number of earthquakes in the case of PWISA, or the smaller number of PISAs, and the appropriate criteria to distinguish them from other potentially similar changes caused by other phenomena.
- Phase III: analysis of these parameters and criteria using a statistically significant number of appropriate samples for one signal.
- Phase IV: appropriate statistical analyses for several transmitters and receivers, which should (a) verify the results obtained in the previous phase and reveal possible differences for different signals and receivers and (b) provide detailed analyses of the observed changes in space.

The development of suitable warning systems can begin only after the potential confirmation of the observed connections, the definition of relevant parameters and criteria for different conditions in the mentioned phases, and the development of software for the automatic detection of defined changes.

Relevant studies on VLF signal changes a few minutes or dozens of minutes before an earthquake are recent (the first paper was published in 2020) and can be considered as pilot studies. In the case of the earthquake precursor analyses during PWISA, there are studies relevant for Phase I and II, and investigations for Phase III are ongoing. In the case of the PISA,

the studies in Phase I are still ongoing. Our plan is to continue this research in all remaining phases, which includes not only analysing the data but also forming a new network of relevant receivers and involving other researchers and/or groups in further work.

It is important to emphasise that there were no significant impacts of other natural phenomena during the observed period. This analysis is given in [29] and refers to the influence of meteorological and geomagnetic conditions. These checks were carried out on the basis of the data presented in [45–47]. In addition, technical problems during reception were excluded in the aforementioned study.

## 5. Conclusions

This study presented an analysis of the VLF signal amplitude in the frequency domain during a period of intense seismic activity in Central Italy, where 907 earthquakes were registered from 26 October to 2 November 2016. The presented research was carried out within the framework of the investigation of new potential earthquake precursors, which manifest themselves in changes in VLF signal amplitude and phase characteristics in the time (reduction of amplitude/phase noise) and frequency (excitation and attenuation of waves at small periods) domains. In general, the contribution of this investigation to the relevant studies on earthquake precursors is the result of the improvement of the observed data time resolution from the usual several dozens of seconds or minutes to 0.1 s. This made it possible to see the following:

- A reduction in the VLF signal amplitude and phase noises;
- The detection of excitations and attenuations of waves at small wave periods, which can be less than 1 s.

These were not observed with the previously used data. These changes started only a few minutes or a few dozens of minutes before an earthquake, which is a significantly more accurate prediction than other methods that detect changes a few days before an earthquake. In addition, the existence of differences in the observed changes indicated the potential possibility of predicting long-term earthquake hazards.

In this study, relevant analyses in the frequency domain related to the seismically active period were presented for the first time. They represented a continuation of the research given for the time domain, in which the changes before earthquakes in that period were already shown in the form of long-term reductions in the amplitude noise.

The results presented in this study were obtained by processing the amplitude values of the signal emitted by the ICV transmitter in Italy and received in Belgrade, Serbia. They showed changes in the observed amplitude characteristics compared to quiet conditions and differences compared to changes observed in periods around earthquakes that did not occur during the period of intensive seismic activity in the localized area. The conclusions of the presented research are as follows:

- Changes in the observed period relative to quiet conditions were visible for small values of the considered wave periods. This is consistent with previous analyses of earthquakes that did not occur under the considered seismic conditions.
- Reduced values of the Fourier amplitude (indicating wave attenuation) were visible in a longer time interval (a longer time interval was observed from 10 October to 10 November). Therefore, it was not possible to determine whether this change was related to seismic activity or caused by some other influence.
- In the domain of wave periods from 1.4 s to 2 s, higher values of the Fourier amplitude (close to the values expected in quiet conditions) were observed compared to its values for near wave periods. This increase was evident during and just before the observed period, indicating the possibility of a link with seismic activity.
- Wave excitations at discrete values of wave periods below 1.5 s, found in previous studies associated with earthquakes that did not occur during intense seismic activity, were not registered.

Even if there is no correlation with seismic activity, it is interesting that the Fourier amplitude for wave periods of less than 5 s increased in the periods around the minimum signal amplitude during sunrise and sunset. These values were much smaller than those recorded during quiet days, which is why the corresponding changes were not observed under quiet conditions.

Since the changes compared to quiet conditions were noticeable and different from those observed in the analyses of earthquakes that did not occur during periods of intense seismic activity, this study indicates the possibility of predicting relevant hazardous periods.

The main limitation of this study is the fact that only one period of intense seismic activity was considered. For this reason, it is necessary to perform the presented analyses for a larger number of these periods in order to obtain statistically significant conclusions and to be able to make a more reliable comparison with changes in VLF signal amplitude characteristics before earthquakes that occur during and outside of these periods. To study the possibility of defining the relevant parameters related to the reduction in the Fourier amplitude and the occurrence of their higher values in certain domains of the wave periods is of utmost importance for the prediction of the duration of the earthquake hazard. For this reason, it is important to point out that it is necessary to include the relevant databases of as many groups as possible in this investigation in order to collect a statistically significant number of these periods.

**Funding:** The author acknowledges funding provided by the Institute of Physics Belgrade through the grants by the Ministry of Education, Science, and Technological Development of the Republic of Serbia.

**Data Availability Statement:** Publicly available datasets were analysed in this study. These data can be found at <http://www.emsc-csem.org/Earthquake/> (accessed on 8 April 2021). The VLF data used for analysis are available from the corresponding author.

**Acknowledgments:** The author is grateful to the editors and unknown reviewers for help in preparing the paper and very useful suggestions and comments.

**Conflicts of Interest:** The author declares no conflict of interest.

## References

1. Boudriki Semlali, B.E.; Molina, C.; Park, H.; Camps, A. On the Correlation Between Earthquakes and Prior Ionospheric Scintillations Over the Ocean: A Study Using GNSS-R Data Between 2017 and 2021. *IEEE J. Sel. Top. Appl.* **2024**, *17*, 2640–2654. [[CrossRef](#)]
2. Huang, Y.; Zhu, P.; Li, S. Feasibility Study on Earthquake Prediction Based on Impending Geomagnetic Anomalies. *Appl. Sci.* **2024**, *14*, 263. [[CrossRef](#)]
3. Hayakawa, M.; Nickolaenko, A.P.; Galuk, Y.P.; Kudintseva, I.G. Manifestations of Nearby Moderate Earthquakes in Schumann Resonance Spectra. *Int. J. Electron. Appl. Res.* **2020**, *7*, 1–28. [[CrossRef](#)]
4. Davies, K.; Baker, D.M. Ionospheric effects observed around the time of the Alaskan earthquake of March 28, 1964. *J. Geophys. Res.* **1965**, *70*, 2251–2253. [[CrossRef](#)]
5. Yuen, P.C.; Weaver, P.F.; Suzuki, R.K.; Furumoto, A.S. Continuous, traveling coupling between seismic waves and the ionosphere evident in May 1968 Japan earthquake data. *J. Geophys. Res.* **1969**, *74*, 2256–2264. [[CrossRef](#)]
6. Calais, E.; Minster, J. GPS, earthquakes, the ionosphere, and the Space Shuttle. *Phys. Earth Planet. Interiors* **1998**, *105*, 167–181. [[CrossRef](#)]
7. Pulinets, S.; Boyarchuk, K. *Ionospheric Precursor of Earthquakes*; Springer: Berlin/Heidelberg, Germany, 2004.
8. Maekawa, S.; Horie, T.; Yamauchi, T.; Sawaya, T.; Ishikawa, M.; Hayakawa, M.; Sasaki, H. A statistical study on the effect of earthquakes on the ionosphere, based on the subionospheric LF propagation data in Japan. *Ann. Geophys.* **2006**, *24*, 2219–2225. [[CrossRef](#)]
9. Sasmal, S.; Chakrabarti, S.K. Ionospheric anomaly due to seismic activities; Part 1: Calibration of the VLF signal of VTX 18.2 KHz station from Kolkata and deviation during seismic events. *Nat. Hazards Earth Syst. Sci.* **2009**, *9*, 1403–1408. [[CrossRef](#)]
10. Chakrabarti, S.K.; Mandal, S.K.; Sasmal, S.; Bhowmick, D.; Choudhury, A.K.; Patra, N.N. First VLF detections of ionospheric disturbances due to Soft Gamma Ray Repeater SGR J1550-5418 and Gamma Ray Burst GRB 090424. *Indian J. Phys.* **2010**, *84*, 1461–1466. [[CrossRef](#)]
11. Oyama, K.I.; Devi, M.; Ryu, K.; Chen, C.H.; Liu, J.Y.; Liu, H.; Bankov, L.; Kodama, T. Modifications of the ionosphere prior to large earthquakes: Report from the Ionosphere Precursor Study Group. *Geosci. Lett.* **2016**, *3*, 6. [[CrossRef](#)]

12. Xiong, P.; Long, C.; Zhou, H.; Battiston, R.; De Santis, A.; Ouzounov, D.; Zhang, X.; Shen, X. Pre-Earthquake Ionospheric Perturbation Identification Using CSES Data via Transfer Learning. *Front. Environ. Sci.* **2021**, *9*, 779255. [[CrossRef](#)]
13. He, L.; Wu, L.; Heki, K.; Guo, C. The Conjugated Ionospheric Anomalies Preceding the 2011 Tohoku-Oki Earthquake. *Front. Earth Sci.* **2022**, *10*, 850078. [[CrossRef](#)]
14. Molina, C.; Boudriki Semlali, B.E.; Park, H.; Camps, A. A Preliminary Study on Ionospheric Scintillation Anomalies Detected Using GNSS-R Data from NASA CYGNSS Mission as Possible Earthquake Precursors. *Remote Sens.* **2022**, *14*, 2555. [[CrossRef](#)]
15. Biagi, P.F.; Piccolo, R.; Ermini, A.; Martellucci, S.; Bellecci, C.; Hayakawa, M.; Capozzi, V.; Kingsley, S.P. Possible earthquake precursors revealed by LF radio signals. *Nat. Hazards Earth Syst. Sci.* **2001**, *1*, 99–104. [[CrossRef](#)]
16. Biagi, P.F.; Maggipinto, T.; Righetti, F.; Loiacono, D.; Schiavulli, L.; Ligonzo, T.; Ermini, A.; Moldovan, I.A.; Moldovan, A.S.; Buyuksarac, A.; et al. The European VLF/LF radio network to search for earthquake precursors: Setting up and natural/man-made disturbances. *Nat. Hazards Earth Syst. Sci.* **2011**, *11*, 333–341. [[CrossRef](#)]
17. Hegai, V.; Kim, V.; Liu, J. The ionospheric effect of atmospheric gravity waves excited prior to strong earthquake. *Adv. Space Res.* **2006**, *37*, 653–659. [[CrossRef](#)]
18. Perrone, L.; De Santis, A.; Abbattista, C.; Alfonsi, L.; Amoruso, L.; Carbone, M.; Cesaroni, C.; Cianchini, G.; De Franceschi, G.; De Santis, A.; et al. Ionospheric anomalies detected by ionosonde and possibly related to crustal earthquakes in Greece. *Ann. Geophys.* **2018**, *36*, 361–371. [[CrossRef](#)]
19. Biagi, P.F.; Piccolo, R.; Ermini, A.; Martellucci, S.; Bellecci, C.; Hayakawa, M.; Kingsley, S.P. Disturbances in LF radio-signals as seismic precursors. *Ann. Geophys.* **2001**, *44*, 1011–1019. [[CrossRef](#)]
20. Molchanov, O.; Hayakawa, M.; Oudoh, T.; Kawai, E. Precursory effects in the subionospheric VLF signals for the Kobe earthquake. *Phys. Earth Planet. Interiors* **1998**, *105*, 239–248. [[CrossRef](#)]
21. Yamauchi, T.; Maekawa, S.; Horie, T.; Hayakawa, M.; Soloviev, O. Subionospheric VLF/LF monitoring of ionospheric perturbations for the 2004 Mid-Niigata earthquake and their structure and dynamics. *J. Atmos. Solar-Terr. Phys.* **2007**, *69*, 793–802. [[CrossRef](#)]
22. Rozhnoi, A.; Solovieva, M.; Molchanov, O.; Hayakawa, M. Middle latitude LF (40 kHz) phase variations associated with earthquakes for quiet and disturbed geomagnetic conditions. *Phys. Chem. Earth Parts A/B/C* **2004**, *29*, 589–598. [[CrossRef](#)]
23. Zhao, S.; Shen, X.; Liao, L.; Zhima, Z.; Zhou, C.; Wang, Z.; Cui, J.; Lu, H. Investigation of Precursors in VLF Subionospheric Signals Related to Strong Earthquakes ( $M > 7$ ) in Western China and Possible Explanations. *Remote Sens.* **2020**, *12*, 3563. [[CrossRef](#)]
24. Maurya, A.K.; Venkatesham, K.; Tiwari, P.; Vijaykumar, K.; Singh, R.; Singh, A.K.; Ramesh, D.S. The 25 April 2015 Nepal Earthquake: Investigation of precursor in VLF subionospheric signal. *J. Geophys. Res. Space Phys.* **2016**, *121*, 10403–10416. [[CrossRef](#)]
25. Boudjada, M.Y.; Biagi, P.F.; Eichelberger, H.U.; Nico, G.; Galopeau, P.H.M.; Ermini, A.; Solovieva, M.; Hayakawa, M.; Lammer, H.; Voller, W.; et al. Analysis of Pre-Seismic Ionospheric Disturbances Prior to 2020 Croatian Earthquakes. *Remote Sens.* **2024**, *16*, 529. [[CrossRef](#)]
26. Biagi, P.; Castellana, L.; Maggipinto, T.; Maggipinto, G.; Minafra, A.; Ermini, A.; Molchanov, O.; Rozhnoi, A.; Solovieva, M.; Hayakawa, M. Anomalies in VLF radio signals related to the seismicity during November–December 2004: A comparison of ground and satellite results. *Phys. Chem. Earth Parts A/B/C* **2009**, *34*, 456–463. [[CrossRef](#)]
27. Nina, A.; Pulnests, S.; Biagi, P.; Nico, G.; Mitrović, S.; Radovanović, M.; Č. Popović, L. Variation in natural short-period ionospheric noise, and acoustic and gravity waves revealed by the amplitude analysis of a VLF radio signal on the occasion of the Kraljevo earthquake ( $M_w = 5.4$ ). *Sci. Total Environ.* **2020**, *710*, 136406. [[CrossRef](#)] [[PubMed](#)]
28. Nina, A.; Nico, G.; Mitrović, S.T.; Čadež, V.M.; Milošević, I.R.; Radovanović, M.; Popović, L.Č. Quiet Ionospheric D-Region (QIonDR) Model Based on VLF/LF Observations. *Remote Sens.* **2021**, *13*, 483. [[CrossRef](#)]
29. Nina, A.; Biagi, P.F.; Pulnests, S.; Nico, G.; Mitrović, S.T.; Čadež, V.M.; Radovanović, M.; Urošev, M.; Popović, L.Č. Variation in the VLF signal noise amplitude during the period of intense seismic activity in Central Italy from 25 October to 3 November 2016. *Front. Environ. Sci.* **2022**, *10*, 1005575. [[CrossRef](#)]
30. Nina, A. Analysis of VLF Signal Noise Changes in the Time Domain and Excitations/Attenuations of Short-Period Waves in the Frequency Domain as Potential Earthquake Precursors. *Remote Sens.* **2024**, *16*, 397. [[CrossRef](#)]
31. Kovačević, A.B.; Nina, A.; Popović, L.Č.; Radovanović, M. Two-Dimensional Correlation Analysis of Periodicity in Noisy Series: Case of VLF Signal Amplitude Variations in the Time Vicinity of an Earthquake. *Mathematics* **2022**, *10*, 4278. [[CrossRef](#)]
32. The Euro-Mediterranean Seismological Centre. Available online: <https://www.emsc-csem.org/> (accessed on 8 April 2021).
33. Hanks, T.C.; Kanamori, H. A moment magnitude scale. *J. Geophys. Res. Solid Earth* **1979**, *84*, 2348–2350. [[CrossRef](#)]
34. Kanamori, H. Magnitude scale and quantification of earthquakes. *Tectonophysics* **1983**, *93*, 185–199. [[CrossRef](#)]
35. Richter, C.F. An instrumental earthquake magnitude scale. *Bull. Seismol. Soc. Am.* **1935**, *25*, 1–32. [[CrossRef](#)]
36. Nina, A.; Simić, S.; Srečković, V.A.; Popović, L.Č. Detection of short-term response of the low ionosphere on gamma ray bursts. *Geophys. Res. Lett.* **2015**, *42*, 8250–8261. [[CrossRef](#)]
37. Wang, J.; Huang, Q.; Ma, Q.; Chang, S.; He, J.; Wang, H.; Zhou, X.; Xiao, F.; Gao, C. Classification of VLF/LF Lightning Signals Using Sensors and Deep Learning Methods. *Sensors* **2020**, *20*, 1030. [[CrossRef](#)] [[PubMed](#)]
38. Thomson, N.R.; Rodger, C.J.; Clilverd, M.A. Large solar flares and their ionospheric D region enhancements. *J. Geophys. Res. Space Phys.* **2005**, *110*, A06306. [[CrossRef](#)]

39. Kolarski, A.; Grubor, D.; Šulić, D. Diagnostics of the Solar X-Flare Impact on Lower Ionosphere through Seasons Based on VLF-NAA Signal Recordings. *Balt. Astron.* **2011**, *20*, 591–595. [[CrossRef](#)]
40. Basak, T.; Chakrabarti, S.K. Effective recombination coefficient and solar zenith angle effects on low-latitude D-region ionosphere evaluated from VLF signal amplitude and its time delay during X-ray solar flares. *Astrophys. Space Sci.* **2013**, *348*, 315–326. [[CrossRef](#)]
41. Schmitter, E.D. Modeling solar flare induced lower ionosphere changes using VLF/LF transmitter amplitude and phase observations at a midlatitude site. *Ann. Geophys.* **2013**, *31*, 765–773. [[CrossRef](#)]
42. Ammar, A.; Ghalila, H. Ranking of Sudden Ionospheric Disturbances by Means of the Duration of VLF Perturbed Signal in Agreement with Satellite X-Ray Flux Classification. *Acta Geophys.* **2016**, *64*, 2794–2809. [[CrossRef](#)]
43. Chakraborty, S.; Basak, T. Numerical analysis of electron density and response time delay during solar flares in mid-litudinal lower ionosphere. *Astrophys. Space Sci.* **2020**, *365*, 1–9. [[CrossRef](#)]
44. Inan, U.S.; Lehtinen, N.G.; Moore, R.C.; Hurley, K.; Boggs, S.; Smith, D.M.; Fishman, G.J. Massive disturbance of the daytime lower ionosphere by the giant  $\gamma$ -ray flare from magnetar SGR 1806-20. *Geophys. Res. Lett.* **2007**, *34*, 8103. [[CrossRef](#)]
45. The European Severe Weather Database. Available online: <https://eswd.eu/cgi-bin/eswd.cgi> (accessed on 28 May 2022).
46. The Helmholtz Centre Potsdam—GFZ German Research Centre for Geosciences. Available online: [https://www-app3.gfz-potsdam.de/kp\\_index/Kp\\_ap\\_Ap\\_SN\\_F107\\_since\\_1932.txt](https://www-app3.gfz-potsdam.de/kp_index/Kp_ap_Ap_SN_F107_since_1932.txt) (accessed on 28 May 2022).
47. The National Aeronautics and Space Administration—NASA. Available online: [https://hesperia.gsfc.nasa.gov/goes/goes\\_event\\_listings/](https://hesperia.gsfc.nasa.gov/goes/goes_event_listings/) (accessed on 28 May 2022).

**Disclaimer/Publisher’s Note:** The statements, opinions and data contained in all publications are solely those of the individual author(s) and contributor(s) and not of MDPI and/or the editor(s). MDPI and/or the editor(s) disclaim responsibility for any injury to people or property resulting from any ideas, methods, instructions or products referred to in the content.